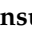







Article

In Vitro Antiviral Effect and Potential Neuroprotection of *Salvadora persica* L. Stem Bark Extract against Lipopolysaccharides-Induced Neuroinflammation in Mice: LC-ESI-MS/MS Analysis of the Methanol Extract

Reem Binsuwaidan ^{1,†}, Walaa A. Negm ^{2,*,†}, Engy Elekhrawy ^{3,*}, Nashwah G. M. Attallah ⁴,
Eman Ahmed ^{5,6}, Sameh Magdeldin ^{6,7}, Ehssan Moglad ⁸, Sally Abdallah Mostafa ⁹
and Suzy A. El-Sherbeni ²

¹ Department of Pharmaceutical Science, College of Pharmacy, Princess Nourah Bint Abdulrahman University, P.O. Box 84428, Riyadh 11671, Saudi Arabia

² Department of Pharmacognosy, Faculty of Pharmacy, Tanta University, Tanta 31527, Egypt

³ Department of Pharmaceutical Microbiology, Faculty of Pharmacy, Tanta University, Tanta 31527, Egypt

⁴ The Egyptian Drug Authority (EDA), Previously NODCAR, Giza 8655, Egypt

⁵ Department of Pharmacology, Faculty of Veterinary Medicine, Suez Canal University, Ismailia 41522, Egypt

⁶ Proteomics and Metabolomics Research Program, Department of Basic Research, Children's Cancer Hospital 57357, Cairo 11441, Egypt

⁷ Department of Physiology, Faculty of Veterinary Medicine, Suez Canal University, Ismailia 41522, Egypt

⁸ Department of Pharmaceutics, College of Pharmacy, Prince Sattam Bin Abdulaziz University, P.O. Box 173, Al-Kharj 11942, Saudi Arabia

⁹ Department of Medical Biochemistry and Molecular Biology, Faculty of Medicine, Mansoura University, Mansoura 35516, Egypt

* Correspondence: walaa.negm@pharm.tanta.edu.eg (W.A.N.); engy.ali@pharm.tanta.edu.eg (E.E.)

† These authors contributed equally to this work.



Citation: Binsuwaidan, R.; Negm, W.A.; Elekhrawy, E.; Attallah, N.G.M.; Ahmed, E.; Magdeldin, S.; Moglad, E.; Mostafa, S.A.; El-Sherbeni, S.A. In Vitro Antiviral Effect and Potential Neuroprotection of *Salvadora persica* L. Stem Bark Extract against Lipopolysaccharides-Induced Neuroinflammation in Mice: LC-ESI-MS/MS Analysis of the Methanol Extract. *Pharmaceuticals* **2023**, *16*, 398. <https://doi.org/10.3390/ph16030398>

Academic Editors: Manuela Leri and Marzia Vasarri

Received: 19 January 2023

Revised: 28 February 2023

Accepted: 3 March 2023

Published: 6 March 2023



Copyright: © 2023 by the authors. Licensee MDPI, Basel, Switzerland. This article is an open access article distributed under the terms and conditions of the Creative Commons Attribution (CC BY) license (<https://creativecommons.org/licenses/by/4.0/>).

Abstract: Neuroinflammation is a serious immunomodulatory complex disorder that causes neurological and somatic ailments. The treatment of brain inflammation with new drugs derived from natural sources is a significant therapeutic goal. Utilizing LC-ESI-MS/MS analysis, the active constituents of *Salvadora persica* extract (SPE) were identified tentatively as exerting antioxidant and anti-inflammatory effects in natural medicine. Herein, we determined the antiviral potential of SPE against herpes simplex virus type 2 (HSV-2) using the plaque assay. HSV-2 is a neurotropic virus that can cause neurological diseases. SPE exhibited promising antiviral potential with a half-maximal cytotoxic concentration (CC₅₀) of 185.960 ± 0.1 µg/mL and a half-maximal inhibitory concentration (IC₅₀) of 8.946 ± 0.02 µg/mL. The in vivo study of the SPE impact against lipopolysaccharide (LPS)-induced neuroinflammation was performed using 42 mice divided into seven groups. All groups were administered LPS (0.25 mg/kg) intraperitoneally, except for the normal and SPE groups 1 and 2. Groups 5, 6, and 7 received 100, 200, and 300 mg/kg SPE. It was revealed that SPE inhibited acetylcholinesterase in the brain. It increased superoxide dismutase and catalase while decreasing malondialdehyde, which explains its antioxidative stress activity. SPE downregulated the gene expression of the inducible nitric oxide synthase, as well as the apoptotic markers (caspase-3 and c-Jun). In addition, it decreased the expression of the proinflammatory cytokines (interleukin-6 and tumor necrosis factor-alpha). Mice administered SPE (300 mg/kg) with LPS exhibited normal neurons in the cerebral cortices, hippocampus pyramidal layer, and cerebellum, as determined by the histopathological analysis. Therefore, using *S. persica* to prevent and treat neurodegeneration could be a promising new therapeutic strategy to be explored.

Keywords: brain; HSV-2; metabolomics; neuroinflammation; oxidative stress; phytoconstituents

1. Introduction

Neuroinflammation is a significant factor that causes many central nervous system (CNS) ailments. It is a complex response to neuronal cell injuries in the brain, including the stimulation of microglia, which are the major cellular components of neuroinflammation. This condition is characterized by the release of proinflammatory cytokines, such as interleukin-6 (IL-6) and tumor necrosis factor- α (TNF α), as well as the production of reactive oxygen species (ROS) and nitric oxide (NO). Neuroinflammation is an innate immune response that acts against infections and variable pathogens. Neurodegenerative and other CNS diseases, including Alzheimer's disease (AD) and Parkinson's (PA), are caused by the proinflammatory mediators mentioned earlier through their contribution to the death of neurons. It is a significant target for treating the neuroinflammation of the brain to manage the severe manifestations of different CNS diseases [1–3].

Arak shrubs belong to the Salvadoraceae family, also known as *Salvadora persica* L. [4,5]. The shrubs are disseminated across the Arabian Peninsula, Africa, and India [6]. It is known that the stems, bark, and roots contain variable secondary metabolites with remarkable free radical scavenging and anti-inflammatory impacts [7]. *S. persica* contains essential oils [8]; flavonoids (such as rutin and quercetin) [9,10]; phenolic acids (such as gallic, chlorogenic, caffeic, and rosmarinic acids) [11]; alkaloids such as persicaline [12]; sulfated glycosides [13]; phenolic diterpenes; salvadourea; benzyl isothiocyanate [14]; chlorides; fluorides; tannins; and fatty acids [9]. It played a significant role in preventing and treating different dental diseases [15]. In addition, it exhibited variable biological activities such as wound healing, analgesic, antimicrobial, antidepressant, anticonvulsant, and anticancer potentials [9]. To discover new drugs for managing neuroinflammation in the various CNS diseases, it is essential to investigate the effects of natural substances such as plants. Interestingly, several plant extracts were found to be effective against the neurodegeneration of AD and PA diseases [16,17].

Many neurotropic viruses can infect the CNS. These viruses, such as herpesviruses, Ebola, and rabies, can lead to multiple nervous system diseases, including meningitis, encephalitis, and flaccid paralysis [18]. Herpesviruses, such as herpes simplex virus type 1 (HSV-1) and HSV-2, are enveloped viruses with double-stranded DNA. They primarily infect the hosts' skin, mucous membranes, and nerve tissues, resulting in high morbidity and mortality rates [19]. Due to their latent neuron infections, HSV-1 and HSV-2 have a high prevalence in the human population, with lifelong infections and sporadic recurrences [20]. Variants of HSV that show resistance to the currently used antivirals are increasing, particularly in immunocompromised patients [21]. Therefore, it is crucial to discover novel antivirals that can decrease the severity and duration of the infections caused by such viruses. In this study, we aimed to investigate the antiviral activity of *Salvadora persica* methanol extract of stem bark (SPE) against the HSV-2 virus.

Since there are insufficient treatments for neurodegenerative disorders, investigating the possibility of using plant extracts as safe and inexpensive sources to prevent and treat such disorders is a promising idea that must be investigated. The present study aimed to investigate the activity of SPE against lipopolysaccharide (LPS)-induced neuroinflammation in mice and assess the underlying mechanism of action and the antiviral activity of SPE against the neurotropic virus HSV-2. In addition, the LC-ESI-MS/MS technique was used to tentatively identify the phytochemical constituents of SPE.

2. Results

2.1. Recognition of the Chemical Profile of *Salvadora persica* Extract by LC-ESI-MS/MS Analysis

The LC-ESI-MS/MS analysis of SPE could represent the phytochemical components and tentatively demonstrate the diversity of its compounds. The presence of phenolic glycosides such as syringin; coumaric acids derivatives (such as rosmarinic acid); phenolic acids (such as sinapic acid); alkyl glucosinolate (such as benzyl glucosinolate); flavonoids (such as kaempferol-7-*O*-neohesperidoside, hesperetin, rhoifolin, and apigenin); and indoles (such as 3-formylindole) displayed the diversity of the components. The major

compounds displayed in negative and positive ESI modes were diosmin, isosakuranetin-7-*O*-neohesperidoside, acacetin-7-*O*-rutinoside, rhoifolin, agmatine, benzyl glucosinolate, hydroxybenzoic acid, spermidine, pantothenate, malic acid, and 3-formylindole, as displayed in Table 1 and Figures 1–3. Figures S1 and S2 depict the negative and positive modes of the total ion chromatogram, respectively.

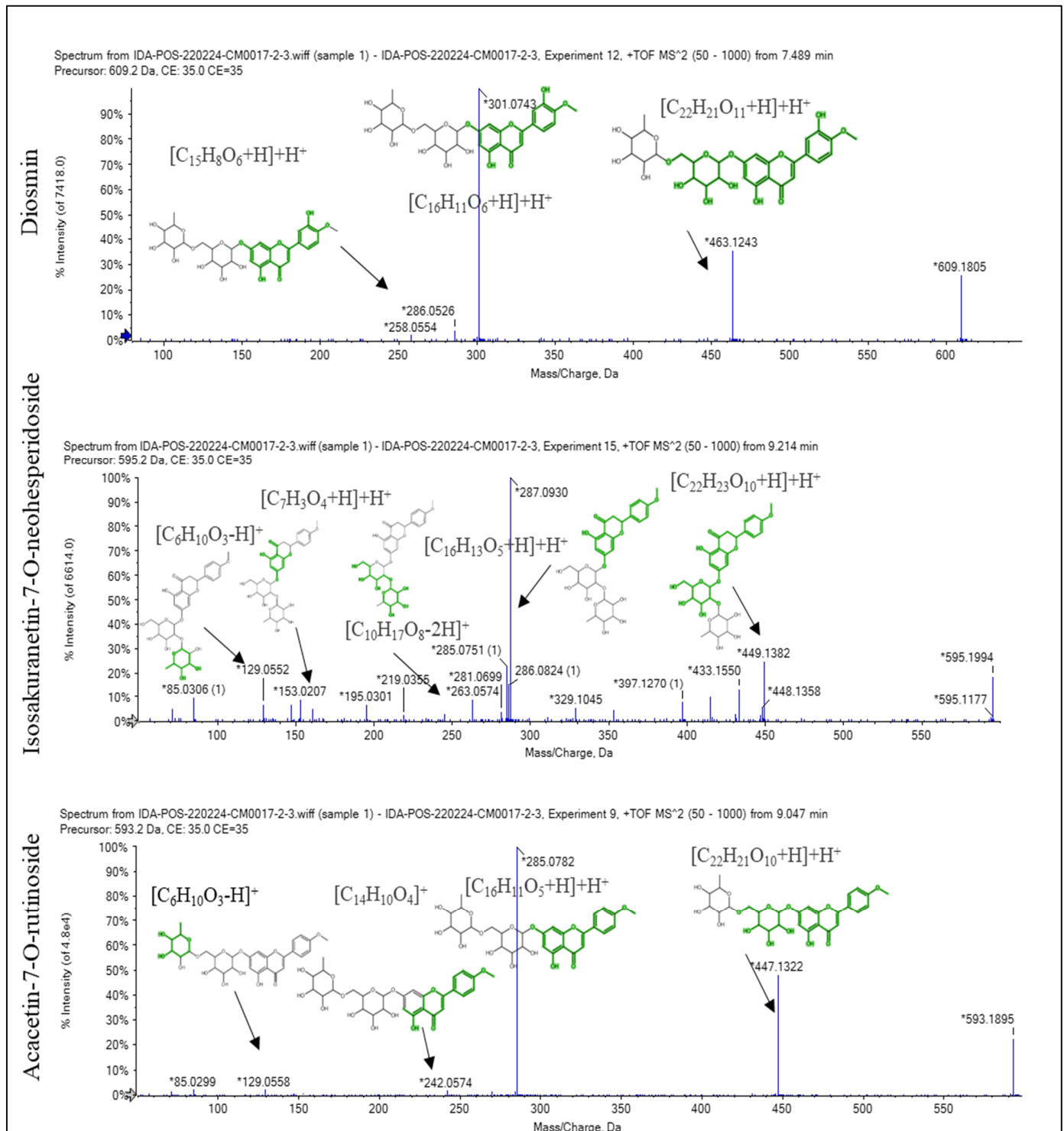


Figure 1. The fragmentation pattern of the main compounds recognized in the methanol extract of *Salvadora persica* stem bark: diosmin, isosakuranetin-7-*O*-neohesperidoside, and acacetin-7-*O*-rutinoside. * stands for m/z of $[M + H]^+$, $[M - H]^-$, and fragments of each compound.

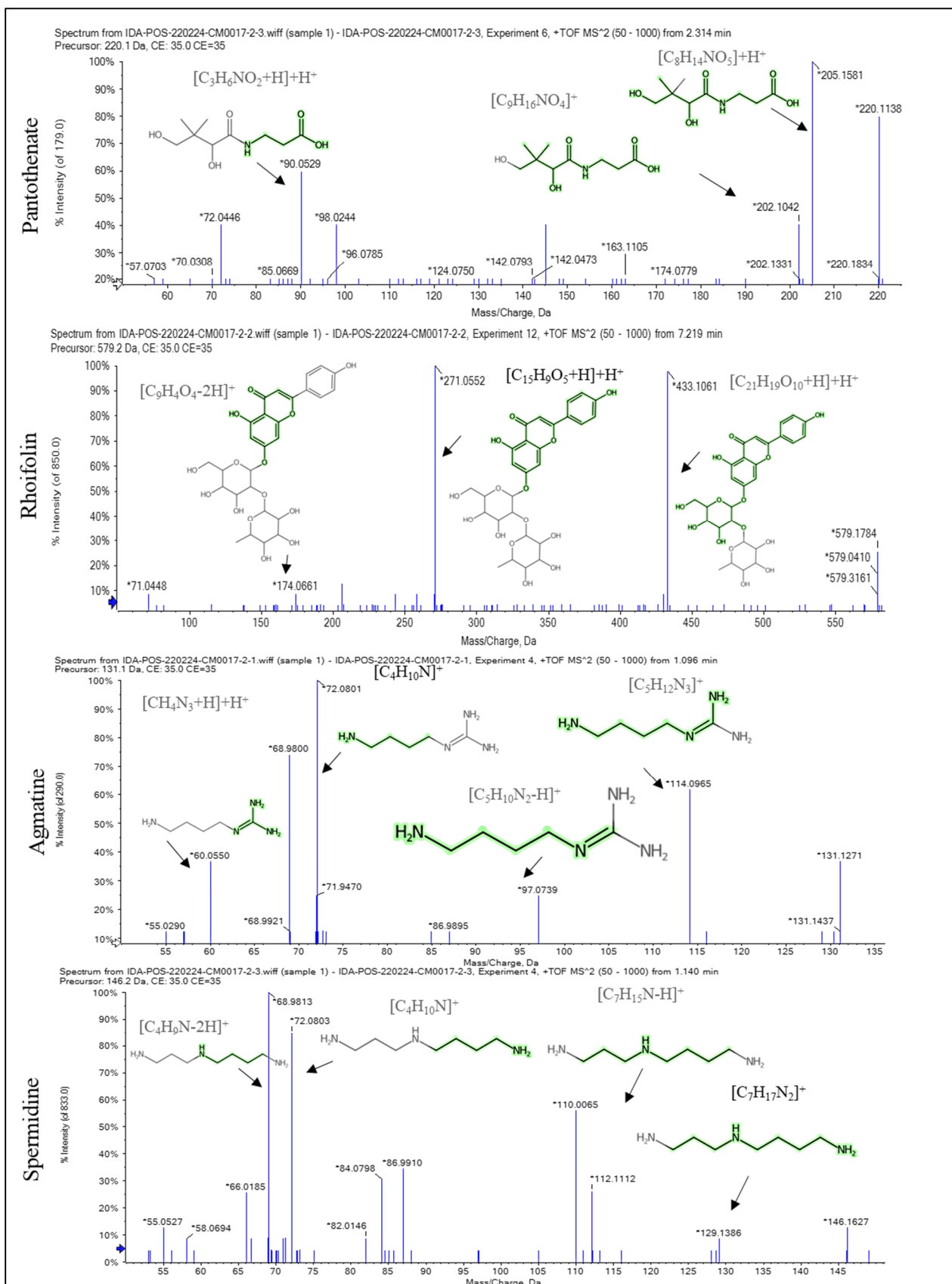


Figure 2. The fragmentation pattern of the main compounds recognized in the methanol extract of *Salvadora persica* stem bark: pantothenate, rhoifolin, agmatine, and spermidine. * stands for m/z of $[M + H]^+$, $[M - H]^+$, and fragments of each compound.

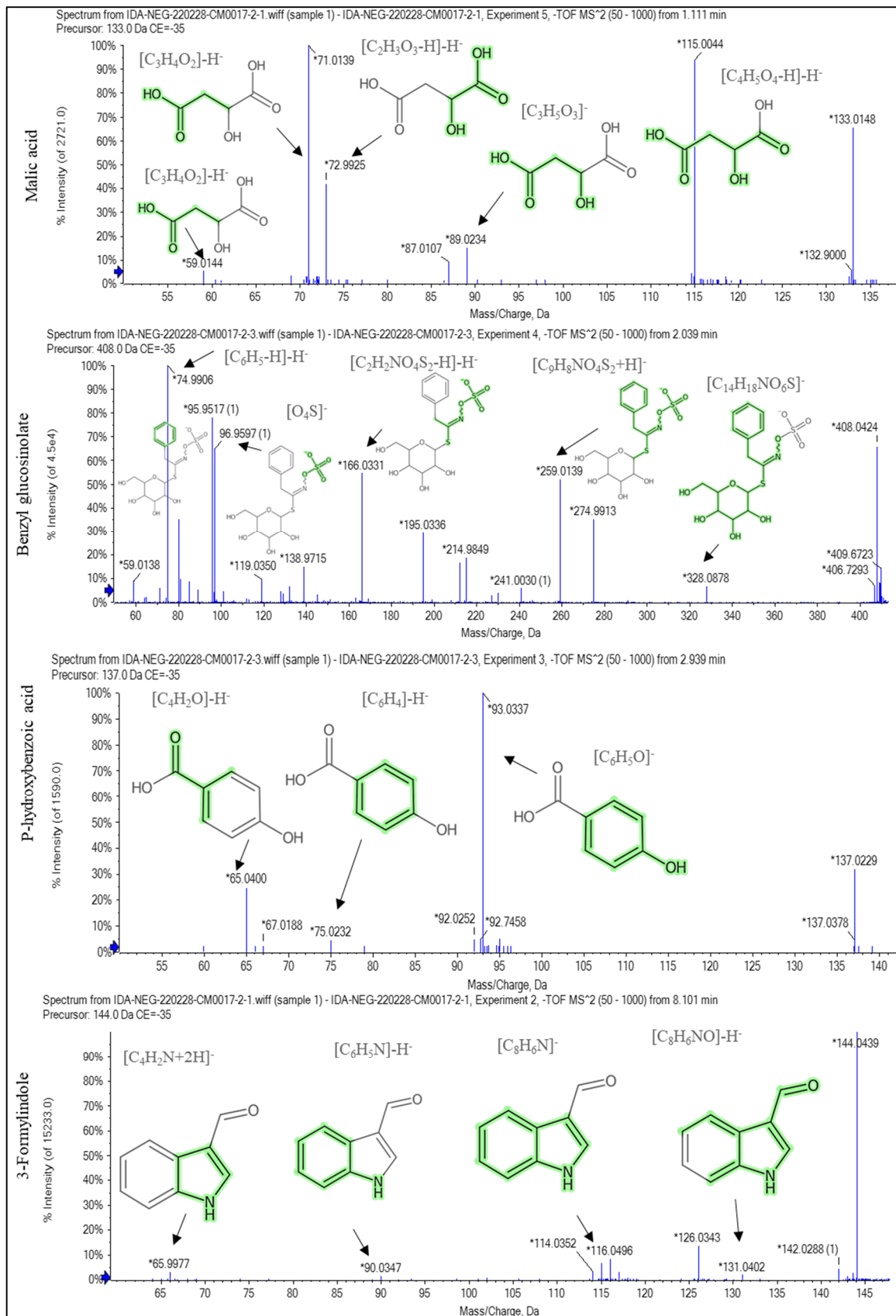


Figure 3. The fragmentation pattern of the main compounds recognized in the methanol extract of *Salvadora persica* stem bark: malic acid, benzyl glucosinolate, p-hydroxy benzoic acid, and 3-formylindole. * stands for m/z of $[M + H]^+$, $[M - H]^-$, and fragments of each compound.

Table 1. LC-ESI-MS/MS analysis of the methanol extract of *Salvadora persica* stem bark displaying the tentatively recognized compounds.

#	RT (min)	Precursor m/z	Error ppm	Compound Name	Formula	Adduction Name	MS/MS	Ontology
1	1.1	131.129	0	Agmatine	C ₅ H ₁₄ N ₄	[M + H] ⁺	60.0550, 72.0801, 114.0965	Guanidines
2	1.12	146.165	0.3	Spermidine	C ₇ H ₁₉ N ₃	[M + H] ⁺	72.0794, 84.08425, 112.1084, 129.1375	Dialkylamines
3	1.15	133.014	−0.6	Malic acid	C ₄ H ₆ O ₅	[M − H] [−]	71.0144, 72.9925, 89.0248, 115.0042	Beta hydroxy acids derivatives
4	1.17	173.045	−0.8	Shikimic acid	C ₇ H ₁₀ O ₅	[M − H] [−]	73.0265, 93.0345, 111.0066, 138.9140, 154.9062	Shikimic acids derivatives
5	1.23	104.107	1.2	Choline	C ₅ H ₁₄ NO	[M] ⁺	58.0660, 60.0816	Cholines
6	1.64	124.039	0.3	Nicotinic acid	C ₆ H ₅ NO ₂	[M + H] ⁺	78.0352, 80.05060, 107.0404	Pyridine carboxylic acids
7	1.65	86.096	−0.3	Piperidine	C ₅ H ₁₁ N	[M + H] ⁺	69.0710, 86.0969	Piperidines
8	2.06	408.042	0.7	Benzyl glucosinolate	C ₁₄ H ₁₉ NO ₉ S ₂	[M − H] [−]	74.9906, 95.9517, 166.0331, 241.0030, 259.0139, 274.9913	Alkylglucosinolates
9	2.33	220.118	−0.6	Pantothenate	C ₉ H ₁₇ NO ₅	[M + H] ⁺	90.0526, 202.1076	Secondary alcohols
10	2.75	167.035	−0.7	Homogenetic acid	C ₈ H ₈ O ₄	[M − H] [−]	108.0210, 109.0304, 122.0345, 123.0485	2(hydroxyphenyl) acetic acids
11	2.93	137.024	−1.8	<i>P</i> -hydroxybenzoic acid	C ₇ H ₆ O ₃	[M − H] [−]	65.0400, 75.0232, 93.0337	Hydroxybenzoic acid derivatives
12	4.38	390.175	−0.3	Syringin	C ₁₇ H ₂₄ O ₉	[M + NH ₄] ⁺	105.0682, 133.0636, 161.0610, 193.0851, 211.0949	Phenolic glycosides
13	4.69	359.077	−0.3	Rosmarinic acid	C ₁₈ H ₁₆ O ₈	[M − H] [−]	72.9911, 123.0408, 133.0296, 161.0247, 179.0321, 197.0480	Coumaric acids derivatives
14	6.26	223.061	0.1	Sinapic acid	C ₁₁ H ₁₂ O ₅	[M − H] [−]	93.0322, 121.0278, 149.0237, 177.0510, 193.0141, 205.0518	Hydroxycinnamic acids
15	6.51	593.151	0.7	Kaempferol-7- <i>O</i> -neohesperidoside	C ₂₇ H ₃₀ O ₁₅	[M − H] [−]	284.0328, 385.0439	Flavonoid-7- <i>O</i> -glycosides
16	6.54	596.173	−0.1	cyanidin-3- <i>O</i> -rutinoside	C ₂₇ H ₃₁ O ₁₅	[M] ⁺	287.0549, 449.1057	Anthocyanidin-3- <i>O</i> -glycosides
17	6.74	301.071	−0.4	Hesperetin	C ₁₆ H ₁₄ O ₆	[M − H] [−]	269.0488, 289.0489, 301.0726	4'- <i>O</i> -methylated flavonoids
18	6.81	181.050	0.7	Syringaldehyde	C ₉ H ₁₀ O ₄	[M − H] [−]	67.0180, 123.0072, 151.0023, 166.0266	Methoxyphenols
19	6.87	167.035	−0.4	5-Methoxysalicylic acid	C ₈ H ₈ O ₄	[M − H] [−]	108.0208, 124.0111, 152.0111	M-methoxybenzoic acids derivatives
20	7.23	579.170	−0.2	Rhoifolin	C ₂₇ H ₃₀ O ₁₄	[M + H] ⁺	271.0579, 433.1155	Flavonoid-7- <i>O</i> -glycosides
21	7.54	609.181	−0.6	Diosmin	C ₂₈ H ₃₂ O ₁₅	[M + H] ⁺	286.0526, 301.0743, 463.1243	Flavonoid-7- <i>O</i> -glycosides
22	7.63	494.141	−0.2	Malvidin-3-galactoside	C ₂₃ H ₂₅ O ₁₂	[M] ⁺	137.0616, 163.0757, 253.0856, 285.1151, 313.1100, 331.1161	Anthocyanidin-3- <i>O</i> -glycosides
23	7.94	174.056	0	1-methoxyindole-3-carbaldehyde	C ₁₀ H ₉ NO ₂	[M − H] [−]	131.0379, 159.0321	Indoles
24	8.02	137.132	−5	Sabinene	C ₁₀ H ₁₆	[M + H] ⁺	65.0379, 94.0376, 122.0327	Bicyclic monoterpenoids
25	8.12	144.045	−1	3-Formylindole	C ₉ H ₇ NO	[M − H] [−]	114.0339, 115.0422, 116.0502, 126.0343, 142.0292	Indoles
26	8.29	177.055	−0.9	Coniferaldehyde	C ₁₀ H ₁₀ O ₃	[M − H] [−]	129.0025, 134.0377, 162.0320	Methoxyphenols
27	8.61	163.040	−0.8	2-Hydroxy cinnamic Acid (2-Coumaric acid)	C ₉ H ₈ O ₃	[M − H] [−]	76.09749, 92.0297, 93.0360, 120.0197	Hydroxycinnamic acids

Table 1. Cont.

#	RT (min)	Precursor m/z	Error ppm	Compound Name	Formula	Adduction Name	MS/MS	Ontology
30	9.08	593.186	−0.2	Acacetin-7-O-rutinoside	C ₂₈ H ₃₂ O ₁₄	[M + H] ⁺	85.0299, 129.0558, 242.0574, 285.0782, 447.1322	Flavonoid-7-O-glycosides
31	9.12	591.171	0.2	Acacetin-7-O-neohesperidoside	C ₂₈ H ₃₂ O ₁₄	[M − H] [−]	268.0378, 283.0612	Flavonoid-7-O-glycosides
32	9.27	595.202	0.8	Isosakuranetin-7-O-neohesperidoside	C ₂₈ H ₃₄ O ₁₄	[M + H] ⁺	85.0306, 129.0552, 153.0207, 195.0301, 263.0574, 287.0930, 433.1550, 449.1382	Flavonoid-7-O-glycosides
33	9.28	287.091	0.7	Isosakuranetin	C ₁₆ H ₁₄ O ₅	[M + H] ⁺	91.0548, 153.0187, 161.0641	4'-O-methylated flavonoids
34	9.78	447.128	0.1	Sissotrin	C ₂₂ H ₂₂ O ₁₀	[M + H] ⁺	149.0152, 242.0657, 270.0481, 285.0748	Isoflavonoid O-glycosides
35	10.51	269.045	0.5	Apigenin	C ₁₅ H ₁₀ O ₅	[M − H] [−]	117.0353, 148.0222, 151.0004, 254.0616	Flavones
36	14.00	285.075	−0.2	Acacetin	C ₁₆ H ₁₂ O ₅	[M + H] ⁺	153.0229, 187.0495, 242.0585, 270.0551	4'-O-methylated flavonoids

2.2. Antiviral Activity

2.2.1. Cytotoxicity of SPE on the Vero-E6 Cells

The values of CC₅₀ of SPE on Vero-E6 cells were determined by the MTT assay, as demonstrated in Figure 4. The value of CC₅₀ was 185.960 ± 0.1 µg/mL. This means that the concentration of SPE that caused death for 50% of the Vero-E6 cells was equal to 185.960 ± 0.1 µg/mL. Thus, we used lower concentrations studying the antiviral activity of SPE on Vero-E6 cells infected with the HSV-2 virus.

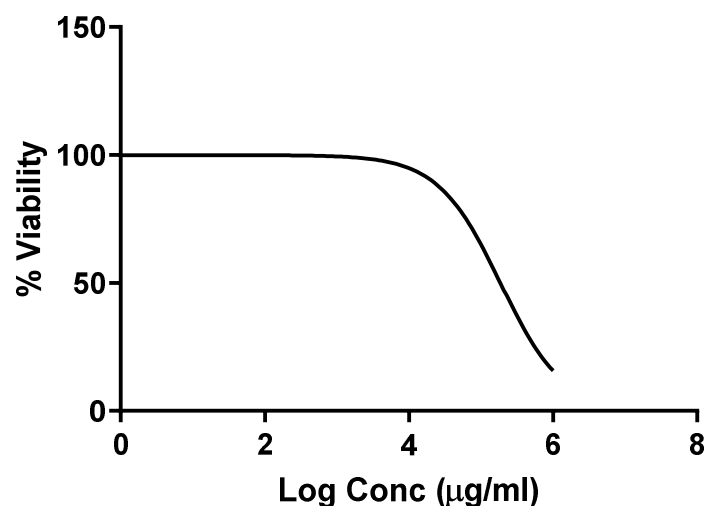


Figure 4. Cytotoxicity curve of *Salvadora persica* methanol extract (CC₅₀ of 185.960 ± 0.1 µg/mL). The results are presented as the mean ± SD.

2.2.2. Antiviral Activity of SPE

The antiviral potential of the SPE was explored against the HSV-2 virus, and the value of the half-maximal inhibitory concentration (IC₅₀) was determined, as shown in Figure 5. The value of IC₅₀ of SPE was 8.946 ± 0.02 µg/mL, and this concentration was needed to inhibit the HSV-2 virus by 50%.

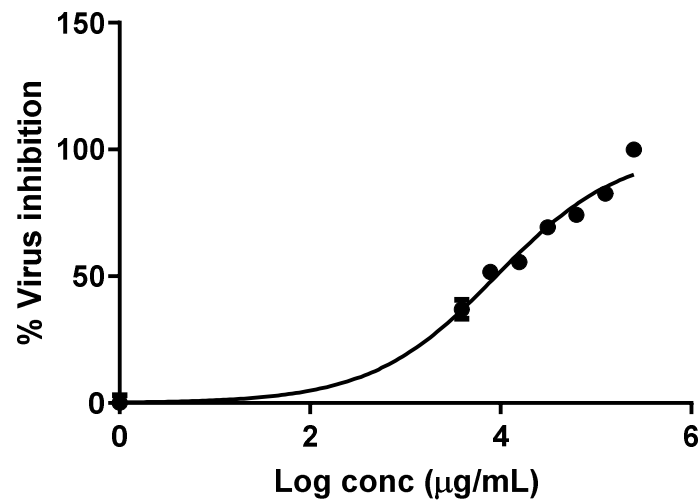


Figure 5. Antiviral activity of *Salvadora persica* methanol extract (IC_{50} of $8.946 \pm 0.02 \mu\text{g/mL}$) against the HSV-2 virus. The results are presented as the mean \pm SD.

2.3. In Vivo Study

2.3.1. Effect on the AChE Activity

LPS significantly increased ($p < 0.05$) the AChE activity compared to the vehicle control. Figure 6 demonstrates that pretreatment with SPE significantly decreased ($p < 0.05$) the increased AChE activity in the brain compared to the LPS-treated group. Groups 5, 6, and 7 revealed a significant decrease ($p < 0.05$) in the AChE activity with percentages of 23.07%, 25%, and 26.9%, respectively.

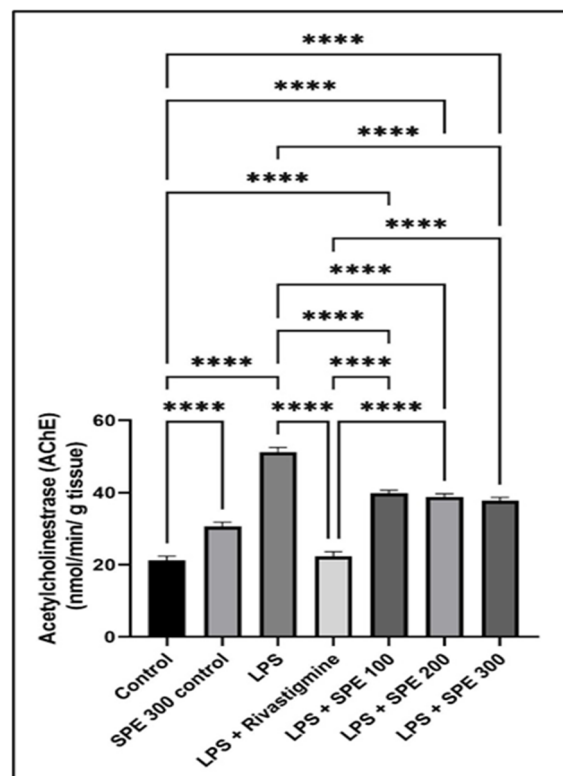


Figure 6. The acetylcholinesterase (AChE) activity of the control (group 1), SPE 300 control (group 2), LPS (group 3), LPS + Rivastigmine (group 4), LPS + SPE 100 (group 5), LPS + SPE 200 (group 6), and LPS + SPE 300 (group 7). ****: Significant at $p \leq 0.0001$.

2.3.2. Effect of SPE on the LPS-Induced Oxidative Stress Markers

Compared to the vehicle control group, LPS significantly increased ($p < 0.05$) the MDA levels, whereas Rivastigmine (RVS) and SPE significantly decreased ($p < 0.05$) the LPS-induced increase in the MDA levels (Figure 7).

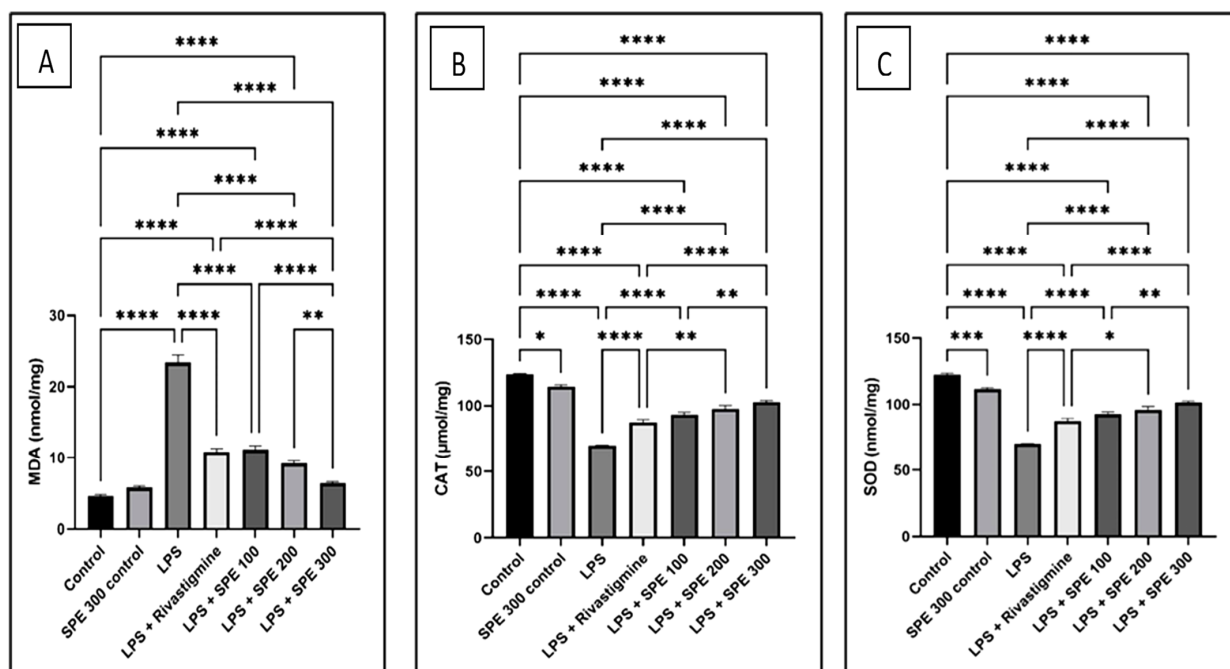


Figure 7. The levels of (A) malondialdehyde (MDA), (B) catalase (CAT), and (C) superoxide dismutase (SOD) of the control (group 1), SPE 300 control (group 2), LPS (group 3), LPS + Rivastigmine (group 4), LPS + SPE 100 (group 5), LPS + SPE 200 (group 6), and LPS + SPE 300 (group 7). *: Significant at $p \leq 0.05$. **: Significant at $p \leq 0.01$. ***: Significant at $p \leq 0.001$. ****: Significant at $p \leq 0.0001$.

The level of oxidative stress induced by LPS administration was evaluated by the CAT and SOD levels in the brain. The levels of CAT and SOD in the LPS-treated group were significantly lower ($p < 0.05$) than the vehicle control group. Compared to the LPS-treated group, the pretreatment with RVS and SPE restored the decreased levels of SOD and CAT (Figure 7).

2.3.3. Effect of SPE on the Relative Gene Expression of IL-6, TNF- α , and iNOS

Compared to the vehicle-treated group, IL-6 gene expression was significantly increased in the LPS-treated group ($p < 0.05$). The significantly low expression levels ($p < 0.05$) of IL-6 in the RVS and SPE pretreated group demonstrated a substantial anti-inflammatory effect in comparison to the LPS-treated group (Figure 8).

Furthermore, the TNF- α and iNOS expression levels were significantly elevated ($p < 0.05$) in the LPS-treated group compared to the vehicle control group. The increased expression of the TNF- α and iNOS levels by LPS was significantly downregulated ($p < 0.05$) by the RVS and SPE pretreatment (Figure 8).

2.3.4. Effect of SPE on the Proapoptotic Gene Expression

In comparison with the vehicle control group, the administration of LPS dramatically increased ($p < 0.05$) the caspase-3 expression level. The increase in the caspase-3 expression levels induced by LPS was considerably reduced ($p < 0.05$) by the RVS and SPE pretreatment.

The c-Jun expression level was substantially higher ($p < 0.05$) after exposure to LPS than in the vehicle control group. Additionally, the c-Jun expression levels were significantly lower ($p < 0.05$) in the RVS and SPE groups (Figure 9).

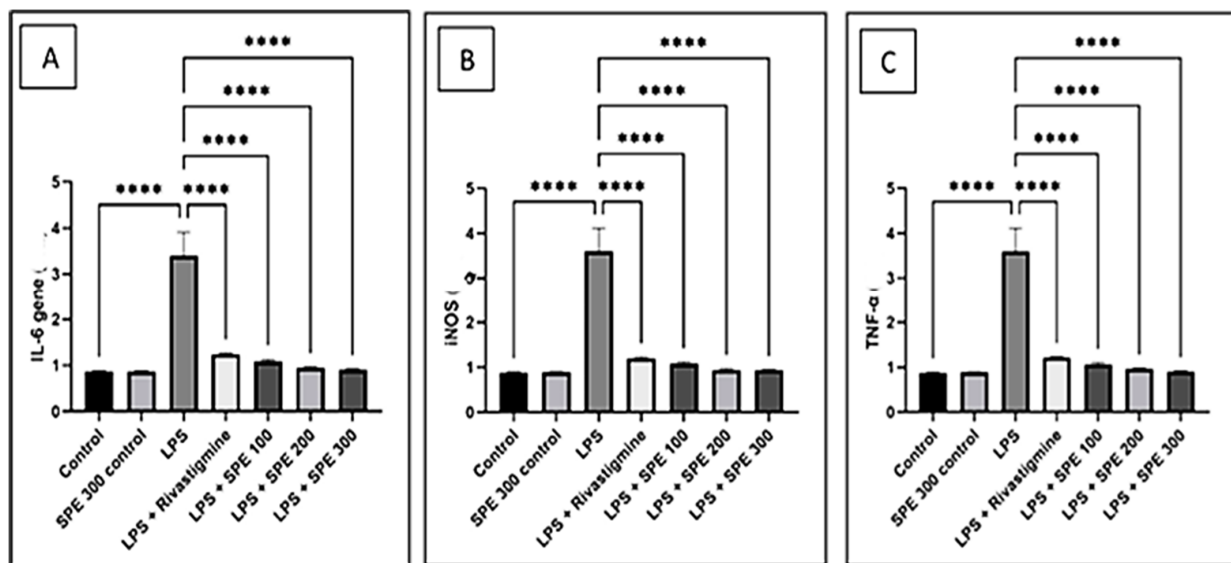


Figure 8. The relative gene expression of (A) interleukin-6 (IL-6), (B) inducible nitric oxide synthase (iNOS), and (C) tumor necrosis factor-alpha (TNF- α) of the control (group 1), SPE 300 control (group 2), LPS (group 3), LPS + Rivastigmine (group 4), LPS + SPE 100 (group 5), LPS + SPE 200 (group 6), and LPS + SPE 300 (group 7). ****: Significant at $p \leq 0.0001$.

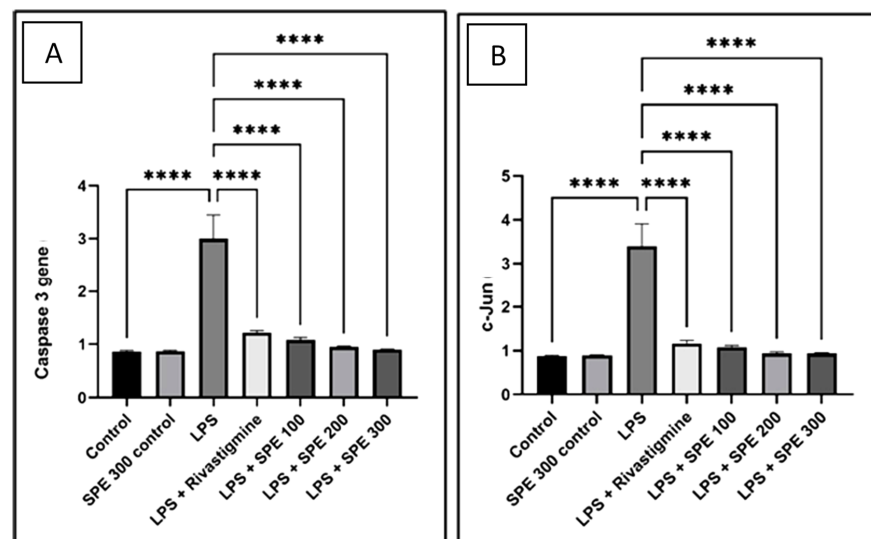


Figure 9. The relative gene expression of (A) caspase-3 and (B) c-Jun of the control (group 1), SPE 300 control (group 2), LPS (group 3), LPS + Rivastigmine (group 4), LPS + SPE 100 (group 5), LPS + SPE 200 (group 6), and LPS + SPE 300 (group 7). **** Significant at $p \leq 0.0001$.

2.3.5. Histopathological Data

Figures 10–12 depict brain sections stained with H&E that illustrate the histopathological characteristics of the various groups in the cerebral cortices, cerebellum, and hippocampus. In the H&E-stained cerebral cortices sections of group 5, there were normal neurons with congested blood vessels. Group 6 exhibited normal neurons with mildly congested blood vessels, while the group 7 sections revealed completely normal neurons. In addition, in the H&E-stained cerebellum sections of group 5, there were markedly degenerated purkinje neurons. Group 6 exhibited a few degenerated purkinje neurons, while the group 7 sections revealed completely normal purkinje neurons. In addition, in the H&E-stained hippocampus sections of groups 5 and 6, there were a few degenerated neurons in the pyramidal layer. Group 7 revealed completely normal neurons in the pyramidal layer.

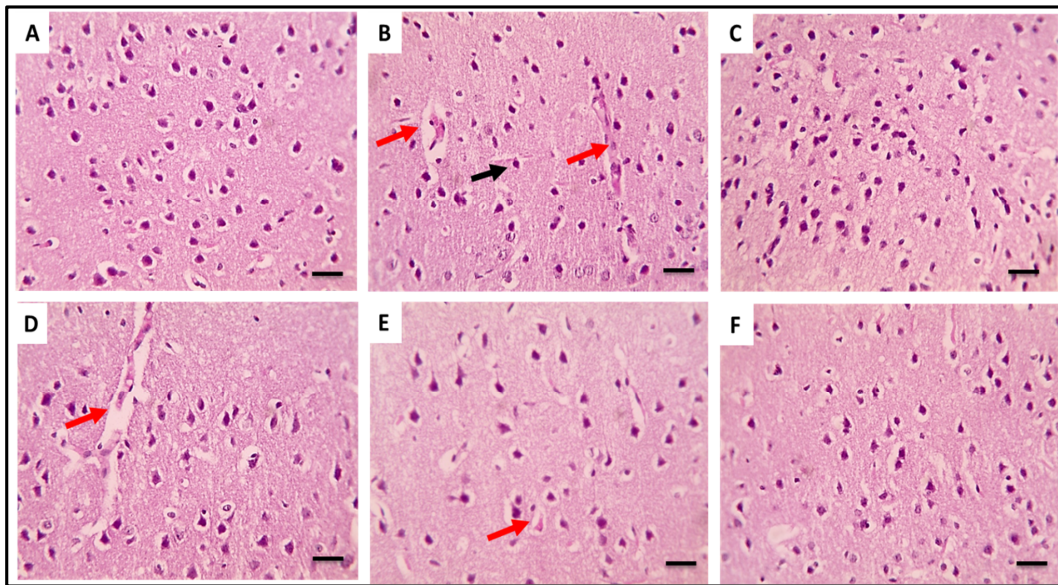


Figure 10. H&E-stained brain sections showing the cerebral cortices of the different groups. Normal neurons were revealed in the control group (group 1, (A)). Sections from the group that received LPS (group 3, (B)) revealed congested blood vessels (red arrows) and the shrinkage of neurons (black arrows). Sections from the treated group with RVS (group 4, (C)) showed normal neurons. Sections from the treated group with SPE 100 mg/kg (group 5, (D)) showed normal neurons with congested blood vessels (red arrow). Sections from the treated group with SPE 200 mg/kg (group 6, (E)) showed normal neurons with mildly congested blood vessels (red arrow). Sections from the treated group with SPE 300 mg/kg (group 7, (F)) showed normal neurons ($\times 400$).

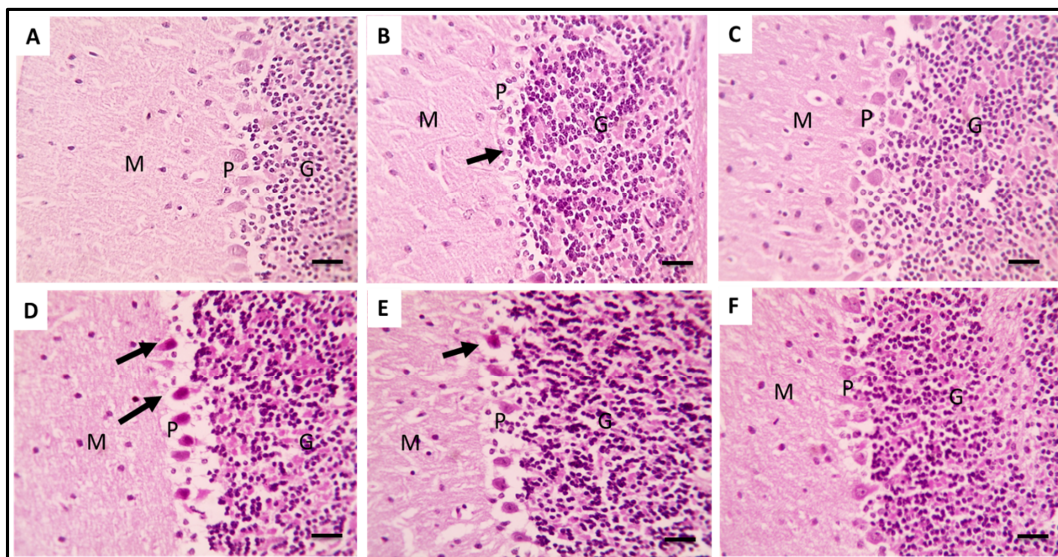


Figure 11. H&E-stained brain sections showing the cerebellum of the different groups. Normal neurons were revealed in the control group (group 1, (A)). Sections from the group that received LPS (group 3, (B)) showed a severe loss of purkinje neurons (black arrow). Sections from the treated group with RVS (group 4, (C)) showed normal purkinje neurons. Sections from the treated group with SPE 100 mg/kg (group 5, (D)) showed markedly degenerated purkinje neurons (black arrows). Sections from the treated group with SPE 200 mg/kg (group 6, (E)) showed a few degenerated purkinje neurons (black arrow). Sections from the treated group with SPE 300 mg/kg (group 7, (F)) showed normal purkinje neurons ($\times 400$). The letters G, P, and M stand for granular layer, purkinje layer, and molecular layer, respectively.

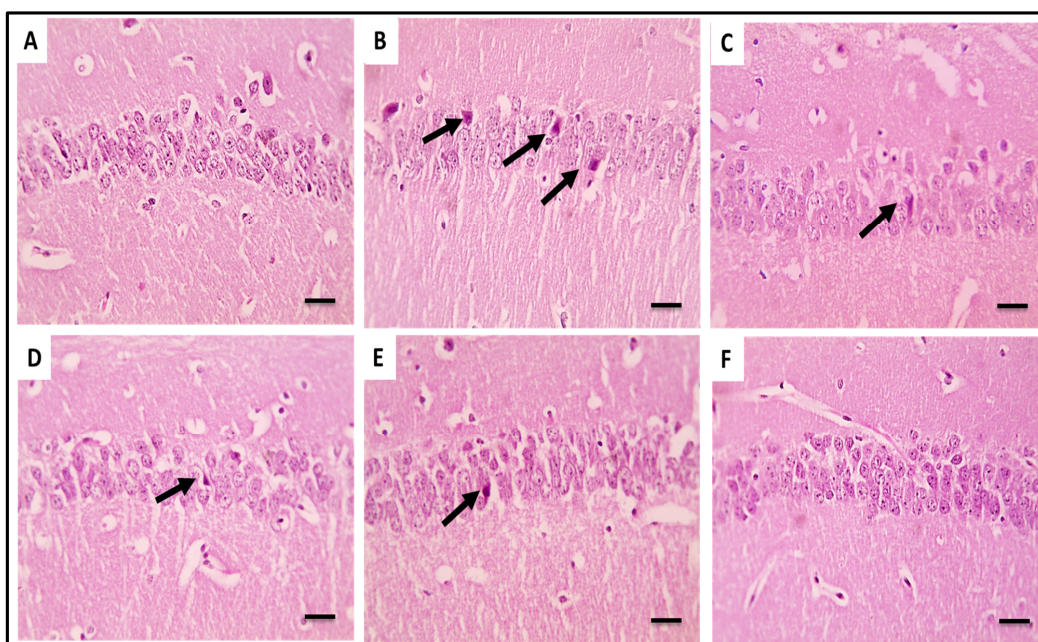


Figure 12. H&E-stained brain sections showing the hippocampus of the different groups. Normal neurons were revealed in the control group (group 1, (A)). Sections from the group that received LPS (group 3, (B)) showed the appearance of many degenerated neurons in the pyramidal layer (black arrows). Sections from the treated group with RVS (group 4, (C)), SPE 100 mg/kg (group 5, (D)), and SPE 200 mg/kg (group 6, (E)) showed the presence of a few degenerated neurons in the pyramidal layer (black arrows). Sections from the treated group with SPE 300 mg/kg showed normal neurons in the pyramidal layer (group 7, (F)) ($\times 400$).

3. Discussion

Neurological disorders are a significant challenge for healthcare systems all over the world. Due to the stressful nature of the current era, these diseases are unfortunately increasing and affecting a large number of people. In addition, treatment options for these diseases are scarce or nonexistent. Most of the used drugs merely alleviate the disease symptoms [22]. Consequently, the discovery of new therapeutic agents for these neurologic diseases is crucial. Plants are considered an abundant source of varieties of bioactive phytochemicals [23], which can be utilized in the treatment of neurological disorders.

In the negative and positive ESI modes, the LC-ESI-MS/MS analysis of SPE revealed 36 compounds of phenolic glycosides, coumaric acids, flavonoids, alkyl glucosinolate, and indoles. Diosmin, isosakuranetin-7-*O*-neohesperidoside (poncirin), acacetin-7-*O*-rutinoside, rhoifolin, agmatine, benzyl glucosinolate, pantothenate, spermidine, hydroxybenzoic acid, malic acid, and 3-formylindole are the most abundant compounds. The neuroprotective effect of diosmin [24] and rhoifolin [25] has been reported in the literature, which may explain the neuroprotective effect of SPE in the current study. In this study, it was found that the SPE contained benzyl glucosinolate. It was revealed that glucosinolate-derived isothiocyanate as benzyl glucosinolate exhibited a broad range of activities against the onset and progression of several neurodegenerative disorders. Glucosinolates have no significant biological effect, but isothiocyanates produced from the hydrolysis of glucosinolates have a neuroprotective effect. The hydrolysis of glucosinolates may be catalyzed by thioglucosidase enzymes present in the gut microbiota of mice, as in humans [26,27]. The ability of isothiocyanates, the activated form of glucosinolate compounds, to improve the endogenous degradation of the protein systems has been investigated as a key protective mechanism to oppose the anomalous build-up of toxic protein oligomers in most neurodegenerative diseases [28]. The reported neuroprotective effect of indole-3-carbinol in PA disease [29] could be used to infer the potential neuroprotective effect of 3-formylindole [29].

Flavonoid-rich foods are significant nutraceuticals that improve health and cognitive capabilities, delay aging, combat chronic diseases, increase life expectancy, and prevent or slow the pathological symptoms of neurodegenerative disorders. Flavonoids may suppress cholinesterases, including AChE, with free-radical scavenging effects and modulation of the signaling pathways included in the cognitive and neuroprotective functions. They increase the vascular blood flow and stimulate neurogenesis. Flavonoids also inhibit apoptosis in neuronal cells [30].

Pantothenate counteracted the pathological effects by preventing disturbances in the glutathione system [31]. Spermidine is a polyamine and an autophagy inducer that can maintain neuronal homeostasis. Healthy brain development and function are dependent on the brain's polyamine concentration. Polyamines interact with the opioid system, glutamatergic signaling, and neuroinflammation in the neuronal and glial compartments. Among the polyamines, spermidine is found at the highest level in the human brain. Age-linked fluctuations in spermidine levels may contribute to impairments in neural networks and neurogenesis. Spermidine has antiaging and anti-inflammatory properties that give protection against neurotoxicity and neurological disorders. Therefore, a polyamine-rich plant extract may be a promising target for increasing the spermidine levels in the brain [32].

HSV-2 is one of the viruses that cause neurological disorders. Therefore, we determined the *in vitro* antiviral activity of SPE against HSV-2 by using the plaque assay. This assay is a standard quantitative method for determining the number of infectious viruses [33]. After allowing serial dilutions of the tested virus to infect cells in the cell culture, this is accomplished by counting the plaques that form in the cell culture [34]. In this study, SPE demonstrated antiviral activity against HSV-2 with a IC_{50} of $8.946 \pm 0.02 \mu\text{g/mL}$. The value of IC_{50} represents the concentration of the tested compound needed to produce 50% inhibition of the studied viruses [34].

Neuroinflammation has been hypothesized to play a role in the development of cognitive impairment and neurodegenerative disorders. Several neurodegenerative diseases, including AD, PA, amyotrophic lateral sclerosis (ALS), and MS (multiple sclerosis), and their specific pathophysiology are unknown. For the study of cognitive impairment associated with neuroinflammation and neurodegenerative diseases, the development of a suitable animal model is essential.

This study aimed to determine how SPE protects mice with LPS-induced neuroinflammation from memory loss and immune reactions. Several studies have demonstrated that the administration of LPS causes neuroinflammation and blood–brain barrier (BBB) damage, followed by amyloid formation and memory loss. In addition, neuronal loss and microglial activation brought on by LPS-induced brain inflammation caused the release of neurotoxic substances, including inflammatory cytokines (TNF- α and IL-6). Chronic LPS administration can impair learning and spatial memory, such as the cognitive loss seen in AD, which is linked to inflammation and amyloid formation due to increased β -amyloid protein (A β) deposition [35–37].

The mechanism by which SPE improved LPS-induced neuroinflammation may be explained by its direct action on the brain via antioxidant and anti-inflammatory effects. The cholinergic system in neuroinflammatory disorders is unbalanced [38]. AChE inhibitors enhance cognition [39] and are the most effective therapy for treating AD patients [40]. LPS increased the activity of AChE in mice brains, which is consistent with a previous study by Tyagi et al. [41]. It caused oxidative damage, decreased acetylcholine (ACh) in the brain [42], and disrupted the cholinergic system by ROS induction [43]. Age-related dementia is correlated with the increase in oxidative stress in the aged population [44]. According to the results of the current experiment, pretreatment with SPE improved the mice's cognitive performance as the SPE (300 mg/kg)-treated group showed a substantial decrease in AChE activity compared to the LPS-treated group.

In addition, H&E-stained brain sections alleviated the detrimental effects of LPS in the cerebral cortices, cerebellum, and hippocampus in the group pretreated with 300 mg/kg SPE.

The process of inflammation is caused by the activation of many inflammatory pathways [45], and several inflammatory mediators, such as iNOS, IL-6, TNF- α , and proapoptotic markers (caspase-3 and c-Jun) are released in this process [46]. Due to its high aerobic metabolism, blood perfusion, and deficient antioxidant defense, the brain is highly susceptible to oxidative damage. As a result, cognitive decline and neuronal damage are attributed to oxidative stress in the brain [47]. Previous research has shown that a mouse's brain underwent a considerable change in oxidative stress indicators after receiving an injection of LPS [48].

Our study found that SPE reduced the proinflammatory mediators and proapoptotic markers in the LPS-induced mice. The MDA levels significantly increased ($p \leq 0.05$) in the brains of the LPS group compared to the normal control group, whereas the CAT and SOD levels significantly decreased ($p \leq 0.05$). Additionally, our findings revealed that SPE administration reversed the aberrant changes in the MDA, SOD, and CAT levels induced by LPS administration. This result demonstrates that the neuroprotective properties of SPE can be attributed to its antioxidant potential. These findings are supported by earlier studies that revealed the ROS-scavenging effects of *S. persica* [48,49].

TNF- α stimulates the production of other cytokines, including IL-6, IL-1, IL-3, etc. Increased A β deposition is linked to the activation of these cytokines. According to several studies, IL-6 and TNF- α are raised by LPS treatments [50,51]. The current research shows that LPS-treated mice have higher TNF- α , IL-6, iNOS, caspase-3, and c-Jun markedly decreased by SPE and rivastigmine pretreatment. Numerous *in vivo* investigations have suggested that inhibiting TNF- α and IL-6 may enhance long-term potentiation and postpone or prevent neuronal dysfunction [52,53]. It has been found that an increase in the caspase-3 levels is related to TNF downstream signaling. These results are supported by research demonstrating a role for caspase-3 in neurodegeneration. Evidence suggests that caspase-3 degrades the tau protein and produces neurofibrillary tangles that impair cognitive function [54]. Similar findings were found in our investigation. SPE administration decreased the LPS-induced production of proinflammatory cytokines, such as TNF- α , IL-6, and iNOS, and apoptotic markers, such as caspase-3 and c-Jun. Hence, SPE prevented LPS-induced neuroinflammation, which prevented memory loss and enhanced cognition. The phosphorylation of tau proteins that causes plaque formation is another process involving JNK 3. As previously reported, c-Jun is the JNK pathway's downstream effector [55], and LPS can activate the c-Jun/JNK pathway, which promotes apoptosis [56]. Our results are consistent with these findings, as the LPS-treated group had elevated c-Jun levels, markedly decreasing the administration of SPE and RVS. As a result, it was proven that SPE had an impact on the apoptosis-related protein c-Jun.

4. Materials and Methods

4.1. Chemicals and Media

All chemicals and media were bought from Merck, the UK, and Oxoid, USA.

4.2. Plant Collection and Preparation of Extract

The fresh stems and twigs barks of *S. persica* shrubs were collected in June 2021 from a farm of Tahoor Freshler Meswak at El-Bagor, Monufia Governorate, Egypt. The plant was identified by Prof. Dr. Mohammed Ibrahim Fotoh, Professor of Ornamental Horticulture and Landscape Design, at the Faculty of Agriculture, Tanta University. The fresh stems and twigs barks (1.5 kg) were dried at room temperature, ground, and extracted with 95% methanol (4 L \times 3 times). The combined extract was evaporated at 40 °C under vacuum to obtain 46.7 g of the extract as a dry residue. A representative sample was kept (PG-A-00522) at the Herbarium of the Department of Pharmacognosy, Faculty of Pharmacy, Tanta University.

4.3. LC-ESI-MS/MS Analysis of SPE

Using LC-ESI-MS/MS and the methodology previously described, the metabolic profile of the defatted methanol extract of *S. persica* stem bark was determined [57,58].

4.4. In Vitro Antiviral Potential

4.4.1. Viruses and Cell Lines

Vero-E6 cells (Vacsera, Cairo, Egypt) were utilized in the propagation of herpes simplex virus type 2 (HSV-2) in Dulbecco's modified Eagle's medium (DMEM) with 10% fetal bovine serum (FBS) and 1% penicillin/streptomycin antibiotics. The viral stocks were generated by inoculating the cells with the viruses in tissue culture flasks and incubating them in an atmosphere containing 5% CO₂ at 37 °C. The tissue culture flasks were inoculated with Vero-E6 cells a day before the virus infection. Trypsin (1%) was added to the infection medium after treating L-1-tosylamido-2-phenylethyl chloromethyl ketone. After two hours of incubation, the medium with the viruses was removed, and a new medium was added and incubated for three days. Following centrifugation to remove cell debris, the supernatant was aliquoted and titrated using the plaque assay [59].

4.4.2. MTT Cytotoxicity Assay

Using 3-(4,5-dimethylthiazol-2-yl)-2,5-diphenyltetrazolium bromide (MTT), the half-maximal cytotoxic concentration (CC50) of SPE was determined [59,60]. The absorbance (A) of the produced formazan was identified at an optical density (OD) of 540 nm using an ELISA reader (Sunrise Tecan, Zürich, Switzerland). The cytotoxicity percentage was calculated according to the equation:

$$\% \text{ cytotoxicity} = \frac{A (\text{cells without treatment}) - A (\text{treated cells})}{A (\text{cells without treatment})} \times 100$$

4.4.3. Plaque Assay

As previously reported [24], it was performed to elucidate the potential antiviral SPE against HSV-2 in a six-well tissue culture plate seeded with Vero-E6 cells (90% confluent). Briefly, after the propagation of the virus, as mentioned earlier, it was 10-fold serially diluted using DMEM. After that, the diluted virus suspension (100 µL) was mixed with DMEM (400 µL), added to the tissue culture plate wells, and incubated at 37 °C. After one hour, the suspension was removed, and the Vero-E6 cells were covered with DMEM supplied with 2% agarose (2%) and the SPE at nontoxic concentrations. The agarose was allowed to solidify, and the tissue culture plates were incubated at 37 °C for 72 h. Subsequently, 10% formalin was added to the well for one hour, removed, and the cells were washed. Finally, 0.1% crystal violet solution was added for staining, and then, the cells were rinsed with water and left to dry. The plaques were enumerated as nonstained spots with a violet background, and the percentage of the inhibition of the plaque formation was calculated using the following equation:

$$\% \text{ inhibition} = \frac{\text{Untreated viral count} - \text{treated viral count}}{\text{untreated viral count}} \times 100$$

4.5. In Vivo Protective Effect against LPS-Induced Neuroinflammation in Mice

4.5.1. Animals

Forty-two adult albino male mice (22–34 g) were used in this study. The animals were maintained in standard laboratory conditions, including 25 ± 2 °C, 60–70% humidity, and free access to food and water. The animals were acclimated for ten days before the trial started [61].

4.5.2. Experimental Groups

The animals were divided randomly into seven groups of six mice each.

Group 1 (vehicle control): mice were administered 0.2 mL saline intraperitoneally (IP).

Group 2: administered only 300 mg/kg of SPE without LPS administration.

Group 3 (negative control or LPS group): mice were administered 0.03 mL of LPS (0.25 mg/kg, IP).

Group 4 (Rivastigmine or RVS group): mice administered RVS (0.25 mg/kg, IP).

Groups 5, 6, and 7: administered SPE in saline at 100, 200, and 300 mg/kg orally.

The treatment period was 28 days, and LPS was administered from days 15 to 21 (groups 3–7). The animals were euthanized on the last day of the previously mentioned period.

4.5.3. Biochemical Assessment

The brains were immediately removed and placed in an extremely cold isotonic solution. The brain was homogenized in phosphate-buffered saline (PBS, pH 7.4). The homogenate was centrifuged at $10,000\times g$ for 15 min, and the supernatant was used for further biochemical analysis.

4.5.3.1. Evaluation of Acetylcholinesterase (AChE) Activity

The activity of AChE reflects both the imbalance in the cholinergic system, as well as the degeneration of the cholinergic neurons in the brain. Briefly, 3 mL of sodium phosphate buffer (0.01 M, pH 8), 50 mL of the supernatant from the brain tissue homogenate, 100 mL of acetyl thio-choline iodide (AcSCh, 0.75 nM), and 100 mL of 5,5'-dithiobis-(2-nitrobenzoic Acid) (DTNB or Ellman's reagent, 10 mM) were mixed. At 412 nm, the absorbance was measured spectrophotometrically every 30 s for 5 min. Micromoles of AcSCh hydrolyzed per min per mg of protein were used to express the results [62].

4.5.3.2. Estimation of Malondialdehyde (MDA) Level

The thiobarbituric acid reactive substances (TBARS) assay was used to quantify MDA, as it can detect the products of lipid oxidation (LPO), as TBARS acts as a source of ROS. This procedure involved incubating 0.1 mL of the brain supernatant with 0.5 mL of Tris-HCl (0.1 M, pH 7.4) for two hours. Following incubation to precipitate the proteins, one milliliter of trichloroacetic acid (TCA) solution (10% *w/v*) was added. The combined product was centrifuged for 10 min with $1000\times g$ at 4 °C. The supernatant was decanted, 0.67% thiobarbituric acid (TBA) was added, and the mixture was placed in boiling water for 15 min. The tubes were immediately placed in an ice bath to cool for 15 min, and then, 1 mL of distilled water was added. A spectrophotometer determined the amount of MDA at 532 nm [63].

4.5.3.3. Estimation of Superoxide Dismutase (SOD) Level

The ability of the enzyme to remove the superoxide radicals created by pyrogallol in an alkaline solution was the basis for measuring the SOD activity. Briefly, 180 mL of potassium phosphate buffer (0.1 M, pH 7.4) and 10 mL of pyrogallol solution were added to 10 L of brain tissue homogenate (2.6 mM in 10 mM HCl). For five minutes, the absorbance increase rate measurements were taken every 30 s. The enzyme needed to block pyrogallol autoxidation by 50% per 200 L of the assay mixture was used to define one unit of SOD [64].

4.5.3.4. Estimation of Catalase (CAT) Level

The CAT level was determined was performed using a biodiagnostics kit (CA 2517, Biodiagnostics, Cairo, Egypt). In brief, the catalase enzyme was allowed to react with a known quantity of H_2O_2 , and after one minute, the reaction was stopped using a catalase inhibitor. The remaining H_2O_2 was combined with 3,5-dichloro-2-hydroxybenzene sulfonic acid (DHBS) and 4-aminophenazone (AAP) in the presence of horseradish peroxidase (HRP) to create a chromophore with a color intensity that was inversely proportional to the quantity of catalase in the initial sample [65].

4.5.3.5. Determination of Caspase-3, Interleukin-6 (IL-6), Tumor Necrosis Factor-Alpha (TNF- α), Inducible Nitric Oxide Synthase (iNOS), and c-Jun Genes Expression by Quantitative Real-Time PCR (qRT-PCR)

TRIzol reagent (Invitrogen, Waltham, USA) was used to purify RNA from the tissue samples. The Maxima first strand cDNA synthesis kit (Thermo Scientific, Waltham, MA, USA) was then used to create complementary DNA (cDNA). The primer sets for genes were produced using the Primer3PLUS program (version 0.4.0; available at <http://frodo.wi.mit.edu> (accessed on 1 December 2022); Table S1). According to the procedure outlined [66], real-time PCR experiments were carried out using the Applied Biosystem 7500 real-time PCR detection system (Life Technologies, San Francisco, CA, USA) using SensiFAST Sybr green Low-Rox PCR master mix kit (Bioline, London, UK). The housekeeping gene was β -actin. In the control group, the relative gene expression for each gene was adjusted to one (negative control) [67].

4.6. Histopathological Analysis

The collected tissue specimens from each group were immediately preserved in 10% formalin. Hematoxylin and eosin (H&E) stains were used to examine the brain sections histopathologically under a light microscope [68].

4.7. Statistics

The results obtained were expressed as mean \pm standard deviation (SD). The in vitro antiviral study used ANOVA and post hoc test (Tukey). Statistical analysis of the in vivo study of each variable was tested for normality using the Shapiro–Wilk normality test. The differences in each variable were analyzed using Kruskal–Wallis, followed by Dunn’s multiple comparisons tests. Statistical analysis was conducted using GraphPad Prism (version 9.3.1, GraphPad, San Diego, CA, USA). The level of statistical significance was set at ($p < 0.05$).

5. Conclusions

The LC-ESI-MS/MS analysis of SPE tentatively demonstrated the diversity of its bioactive compounds. Diosmin, isosakuranetin-7-*O*-neohesperidoside, acacetin-7-*O*-rutinoside, rhoifolin, spermidine, pantothenate, benzyl glucosinolate, hydroxybenzoic acid, and 3-formylindole were the most abundant compounds. These components may account for *Salvadora persica*’s anti-inflammatory and antioxidant properties. This study demonstrated that SPE possessed antiviral activity against HSV-2, the causative agent of certain neurological disorders. Additionally, SPE reduced the brain inflammation caused by LPs. The decrease in the MDA levels and the increase in the SOD and CAT levels demonstrated the ability of SPE to inhibit oxidative stress. It exhibited anti-neuroinflammatory and antiapoptotic properties by decreasing the LPS-induced production of proinflammatory cytokines such as TNF-, IL-6, and iNOS. SPE enhanced the cognitive performance of mice due to a significant decrease in AChE activity compared to the LPS-treated group. At 300 mg/kg of SPE, normal neurons appeared in the cerebral cortices, cerebellum, and hippocampus. Therefore, it should be considered that SPE could be used for prophylaxis and to treat neurodegenerative diseases caused by inflammatory or oxidative damage.

Supplementary Materials: The following supporting information can be downloaded at: <https://www.mdpi.com/article/10.3390/ph16030398/s1>: Figure S1: Total ion chromatogram (negative mode) of LC-ESI-MS/MS of methanol extract of *Salvadora persica* stem bark. Figure S2: Total ion chromatogram (positive mode) of LC-ESI-MS/MS of methanol extract of *Salvadora persica* stem bark. Table S1: Primer sequences of the tested genes.

Author Contributions: Conceptualization, W.A.N., E.E. and S.A.E.-S.; Formal analysis, R.B., E.A. and S.M.; Funding acquisition, R.B. and N.G.M.A.; Investigation, E.A., S.M., W.A.N., E.E. and S.A.E.-S.; Methodology, W.A.N., E.E., S.A.M. and S.A.E.-S.; Resources, E.A. and S.M.; Software, R.B. and N.G.M.A.; Validation, N.G.M.A.; Writing—original draft, W.A.N., E.E., S.A.M. and S.A.E.-S.; and Writing—review and editing, W.A.N., E.E., E.M., S.A.M. and S.A.E.-S. All authors have read and agreed to the published version of the manuscript.

Funding: This research was funded by Princess Nourah bint Abdulrahman University Researchers Supporting Project number (PNURSP2023R304), Princess Nourah bint Abdulrahman University, Riyadh, Saudi Arabia.

Institutional Review Board Statement: The research ethics committee of the Faculty of Pharmacy, Tanta University, Egypt, approved the experiment (TP/RE/1/23p-002).

Informed Consent Statement: Not applicable.

Data Availability Statement: The authors confirm that the data supporting this study are available within the article and Supplementary Files.

Acknowledgments: We thank Princess Nourah bint Abdulrahman University Researchers Supporting Project number (PNURSP2023R304), Princess Nourah bint Abdulrahman University, Riyadh, Saudi Arabia for supporting our project.

Conflicts of Interest: The authors declare no conflict of interest.

References

1. Mukhara, D.; Oh, U.; Neigh, G.N. Neuroinflammation. *Handb. Clin. Neurol.* **2020**, *175*, 235–259. [PubMed]
2. Hopper, A.T.; Campbell, B.M.; Kao, H.; Pintchovski, S.A.; Staal, R.G. Recent developments in targeting neuroinflammation in disease. *Annu. Rep. Med. Chem.* **2012**, *47*, 37–53.
3. Sarker, S.D.; Nahar, L. *Medicinal Natural Products: A Disease-Focused Approach*; Academic Press: Cambridge, MA, USA, 2020.
4. Khatak, M.; Khatak, S.; Siddiqui, A.; Vasudeva, N.; Aggarwal, A.; Aggarwal, P. *Salvadora persica*. *Pharmacogn. Rev.* **2010**, *4*, 209–214. [CrossRef]
5. Khan, A.L.; Asaf, S.; Lubna; Al-Rawahi, A.; Al-Harrasi, A. Decoding first complete chloroplast genome of toothbrush tree (*Salvadora persica* L.): Insight into genome evolution, sequence divergence and phylogenetic relationship within Brassicales. *BMC Genom.* **2021**, *22*, 312. [CrossRef] [PubMed]
6. Mansour, H.; Alsamadany, H.; Al-Hasawi, Z.M. Genetic diversity and genetic structure of *Salvadora persica* L., rare plant species in Rabigh province, Saudi Arabia: Implications for conservation. *J. Taibah Univ. Sci.* **2020**, *14*, 881–888. [CrossRef]
7. Mekhemar, M.; Geib, M.; Kumar, M.; Hassan, Y.; Dörfer, C. *Salvadora persica*: Nature’s gift for periodontal health. *Antioxidants* **2021**, *10*, 712. [CrossRef]
8. Alali, F.; Hudaib, M.; Aburjai, T.; Khairallah, K.; Al-Hadidi, N. GC-MS Analysis and Antimicrobial Activity of the Essential Oil from the Stem of the Jordanian Toothbrush Tree *Salvadora persica*. *Pharm. Biol.* **2005**, *42*, 577–580. [CrossRef]
9. Kumar, D.; Sharma, P.K. Traditional use, phytochemicals and pharmacological activity of *Salvadora persica*: A Review. *Curr. Nutr. Food Sci.* **2021**, *17*, 302–309. [CrossRef]
10. Owis, A.I.; El-Hawary, M.S.; El Amir, D.; Refaat, H.; Alaaeldin, E.; Aly, O.M.; Elrehany, M.A.; Kamel, M.S. Flavonoids of *Salvadora persica* L.(meswak) and its liposomal formulation as a potential inhibitor of SARS-CoV-2. *RSC Adv.* **2021**, *11*, 13537–13544. [CrossRef]
11. Ibrahim, I.I.; Moussa, A.A.; Chen, Z.; Zhang, J.; Cao, W.G.; Yu, C. Bioactive phenolic components and antioxidant activities of water-based extracts and flavonoid-rich fractions from *Salvadora persica* L. leaves. *Nat. Prod. Res.* **2022**, *36*, 2591–2594. [CrossRef]
12. Farag, M.; Abdel-Mageed, W.M.; Basudan, O.; El-Gamal, A. Persicaline, a new antioxidant sulphur-containing imidazoline alkaloid from *Salvadora persica* roots. *Molecules* **2018**, *23*, 483. [CrossRef] [PubMed]
13. Ohtani, K.; Kasai, R.; Yamasaki, K.; Tanaka, O.; Kamel, M.; Assaf, M.; El-Shanawani, M.; Ali, A. Lignan glycosides from stems of *Salvadora persica*. *Phytochemistry* **1992**, *31*, 2469–2471. [CrossRef]
14. Sofrata, A.; Santangelo, E.M.; Azeem, M.; Borg-Karlson, A.K.; Gustafsson, A.; Pütsep, K. Benzyl isothiocyanate, a major component from the roots of *Salvadora persica* is highly active against Gram-negative bacteria. *PLoS ONE* **2011**, *6*, e23045. [CrossRef] [PubMed]
15. Haque, M.M.; Alsareii, S.A. A review of the therapeutic effects of using miswak (*Salvadora persica*) on oral health. *Saudi Med. Med. J.* **2015**, *36*, 530. [CrossRef]
16. Feng, S.T.; Wang, Z.Z.; Yuan, Y.H.; Sun, H.M.; Chen, N.H.; Zhang, Y. Mangiferin: A multipotent natural product preventing neurodegeneration in Alzheimer’s and Parkinson’s disease models. *Pharmacol. Res.* **2019**, *146*, 104336. [CrossRef]
17. Wu, X.; Yan, Y.; Zhang, Q. Neuroinflammation and Modulation Role of Natural Products after Spinal Cord Injury. *J. Inflamm. Res.* **2021**, *14*, 5713–5737. [CrossRef] [PubMed]

18. Bello-Morales, R.; Andreu, S.; López-Guerrero, J.A. The role of herpes simplex virus type 1 infection in demyelination of the central nervous system. *Int. J. Mol. Sci.* **2020**, *21*, 5026. [[CrossRef](#)] [[PubMed](#)]
19. Verzosa, A.L.; McGeever, L.A.; Bhark, S.-J.; Delgado, T.; Salazar, N.; Sanchez, E.L. Herpes simplex virus 1 infection of neuronal and non-neuronal cells elicits specific innate immune responses and immune evasion mechanisms. *Front. Immunol.* **2021**, *12*, 644664. [[CrossRef](#)]
20. Álvarez, D.M.; Castillo, E.; Duarte, L.F.; Arriagada, J.; Corrales, N.; Fariás, M.A.; Henríquez, A.; Agurto-Muñoz, C.; González, P.A. Current antivirals and novel botanical molecules interfering with herpes simplex virus infection. *Front. Microbiol.* **2020**, *11*, 139. [[CrossRef](#)]
21. Dong, H.; Wang, Z.; Zhao, D.; Leng, X.; Zhao, Y. Antiviral strategies targeting herpesviruses. *J. Virus Virus Erad.* **2021**, *7*, 100047. [[CrossRef](#)]
22. Pohl, F.; Kong Thoo Lin, P. The potential use of plant natural products and plant extracts with antioxidant properties for the prevention/treatment of neurodegenerative diseases: In vitro, in vivo and clinical trials. *Molecules* **2018**, *23*, 3283. [[CrossRef](#)] [[PubMed](#)]
23. Binsuwaidan, R.; Sultan, A.A.; Negm, W.A.; Attallah, N.G.; Alqahtani, M.J.; Hussein, I.A.; Shaldam, M.A.; El-Sherbeni, S.A.; Elekhawwy, E. Bilosomes as nanopatform for oral delivery and modulated in vivo antimicrobial activity of lycopene. *Pharmaceuticals* **2022**, *15*, 1043. [[CrossRef](#)] [[PubMed](#)]
24. Habib, C.N.; Mohamed, M.R.; Tadros, M.G.; Tolba, M.F.; Menze, E.T.; Masoud, S.I. The potential neuroprotective effect of diosmin in rotenone-induced model of Parkinson's disease in rats. *Eur. J. Pharmacol.* **2022**, *914*, 174573. [[CrossRef](#)]
25. Brinza, I.; Abd-Alkhalik, A.M.; El-Raey, M.A.; Boiangiu, R.S.; Eldahshan, O.A.; Hritcu, L. Ameliorative effects of rhoifolin in scopolamine-induced amnesic zebrafish (*Danio rerio*) model. *Antioxidants* **2020**, *9*, 580. [[CrossRef](#)] [[PubMed](#)]
26. Halkier, B.A.; Gershenzon, J. Biology and biochemistry of glucosinolates. *Annu. Rev. Plant Biol.* **2006**, *57*, 303–333. [[CrossRef](#)]
27. Verkerk, R.; Schreiner, M.; Krumbein, A.; Ciska, E.; Holst, B.; Rowland, I.; De Schrijver, R.; Hansen, M.; Gerhäuser, C.; Mithen, R. Glucosinolates in Brassica vegetables: The influence of the food supply chain on intake, bioavailability and human health. *Mol. Nutr. Food Res.* **2009**, *53*, S219. [[CrossRef](#)]
28. Angeloni, C.; Hrelia, S.; Malaguti, M. Neuroprotective effects of Glucosinolates. In *Glucosinolates*; Springer: Berlin/Heidelberg, Germany, 2017; pp. 275–299.
29. Mohamad, K.A.; El-Naga, R.N.; Wahdan, S.A. Neuroprotective effects of indole-3-carbinol on the rotenone rat model of Parkinson's disease: Impact of the SIRT1-AMPK signaling pathway. *Toxicol. Appl. Pharmacol.* **2022**, *435*, 115853. [[CrossRef](#)]
30. Ayaz, M.; Sadiq, A.; Junaid, M.; Ullah, F.; Ovais, M.; Ullah, I.; Ahmed, J.; Shahid, M. Flavonoids as prospective neuroprotectants and their therapeutic propensity in aging associated neurological disorders. *Front. Aging Neurosci.* **2019**, *11*, 155. [[CrossRef](#)]
31. Slyshenkov, V.S.; Shevalye, A.A.; Moiseenok, A.G. Pantothenate prevents disturbances in the synaptosomal glutathione system and functional state of synaptosomal membrane under oxidative stress conditions. *Neurochem. J.* **2007**, *1*, 235–239. [[CrossRef](#)]
32. Ghosh, I.; Sankhe, R.; Mudgal, J.; Arora, D.; Nampoothiri, M. Spermidine, an autophagy inducer, as a therapeutic strategy in neurological disorders. *Neuropeptides* **2020**, *83*, 102083. [[CrossRef](#)]
33. Ács, N.; Gambino, M.; Brøndsted, L. Bacteriophage enumeration and detection methods. *Front. Microbiol.* **2020**, *11*, 2662. [[CrossRef](#)] [[PubMed](#)]
34. Mendoza, E.J.; Manguiat, K.; Wood, H.; Drebot, M. Two detailed plaque assay protocols for the quantification of infectious SARS-CoV-2. *Curr. Protoc. Microbiol.* **2020**, *57*, cpmc105. [[CrossRef](#)] [[PubMed](#)]
35. Cummings, J.L. Alzheimer's disease. *N. Engl. J. Med.* **2004**, *351*, 56–67. [[CrossRef](#)]
36. Qin, L.; Wu, X.; Block, M.L.; Liu, Y.; Breese, G.R.; Hong, J.S.; Knapp, D.J.; Crews, F.T. Systemic LPS causes chronic neuroinflammation and progressive neurodegeneration. *Glia* **2007**, *55*, 453–462. [[CrossRef](#)]
37. Alotaibi, B.; Mokhtar, F.A.; El-Masry, T.A.; Elekhawwy, E.; Mostafa, S.A.; Abdelkader, D.H.; Elharty, M.E.; Saleh, A.; Negm, W.A. Antimicrobial activity of *Brassica rapa* L. flowers extract on gastrointestinal tract infections and antiulcer potential against indomethacin-induced gastric ulcer in rats supported by metabolomics profiling. *J. Inflamm. Res.* **2021**, *14*, 7411. [[CrossRef](#)]
38. Alexandris, A.; Walker, L.; Liu, A.; McAleese, K.; Johnson, M.; Pearce, R.; Gentleman, S.; Attems, J. Cholinergic deficits and galaninergic hyperinnervation of the nucleus basalis of Meynert in Alzheimer's disease and Lewy body disorders. *Neuropathol. Appl. Neurobiol.* **2020**, *46*, 264–278. [[CrossRef](#)]
39. Eldufani, J.; Blaise, G. The role of acetylcholinesterase inhibitors such as neostigmine and rivastigmine on chronic pain and cognitive function in aging: A review of recent clinical applications. *Alzheimer's Dement. Transl. Res. Clin. Interv.* **2019**, *5*, 175–183. [[CrossRef](#)] [[PubMed](#)]
40. Saify, Z.S.; Sultana, N. Role of acetylcholinesterase inhibitors and Alzheimer Disease. In *Drug Design and Discovery in Alzheimer's Disease*; Elsevier: Amsterdam, The Netherlands, 2014; pp. 387–425.
41. Tyagi, E.; Agrawal, R.; Nath, C.; Shukla, R. Influence of LPS-induced neuroinflammation on acetylcholinesterase activity in rat brain. *J. Neuroimmunol.* **2008**, *205*, 51–56. [[CrossRef](#)] [[PubMed](#)]
42. Tyagi, E.; Agrawal, R.; Nath, C.; Shukla, R. Effect of melatonin on neuroinflammation and acetylcholinesterase activity induced by LPS in rat brain. *Eur. J. Pharmacol.* **2010**, *640*, 206–210. [[CrossRef](#)]

43. Bargi, R.; Asgharzadeh, F.; Beheshti, F.; Hosseini, M.; Sadeghnia, H.R.; Khazaei, M. The effects of thymoquinone on hippocampal cytokine level, brain oxidative stress status and memory deficits induced by lipopolysaccharide in rats. *Cytokine* **2017**, *96*, 173–184. [[CrossRef](#)]
44. Ton AM, M.; Campagnaro, B.P.; Alves, G.A.; Aires, R.; Côco, L.Z.; Arpini, C.M.; Guerra e Oliveira, T.; Campos-Toimil, M.; Meyrelles, S.S.; Pereira TM, C. Oxidative stress and dementia in Alzheimer's patients: Effects of synbiotic supplementation. *Oxidative Med. Cell. Longev.* **2020**, *2020*, 2638703. [[CrossRef](#)]
45. Yu, Y.; Shen, Q.; Lai, Y.; Park, S.Y.; Ou, X.; Lin, D.; Jin, M.; Zhang, W. Anti-inflammatory effects of curcumin in microglial cells. *Front. Pharmacol.* **2018**, *9*, 386. [[CrossRef](#)] [[PubMed](#)]
46. Cheng, P.; Wang, T.; Li, W.; Muhammad, I.; Wang, H.; Sun, X.; Yang, Y.; Li, J.; Xiao, T.; Zhang, X. Baicalin alleviates lipopolysaccharide-induced liver inflammation in chicken by suppressing TLR4-mediated NF- κ B pathway. *Front. Pharmacol.* **2017**, *8*, 547. [[CrossRef](#)] [[PubMed](#)]
47. Bhat, A.H.; Dar, K.B.; Anees, S.; Zargar, M.A.; Masood, A.; Sofi, M.A.; Ganie, S.A. Oxidative stress, mitochondrial dysfunction and neurodegenerative diseases; a mechanistic insight. *Biomed. Pharmacother.* **2015**, *74*, 101–110. [[CrossRef](#)] [[PubMed](#)]
48. Zhang, X.-Y.; Cao, J.-B.; Zhang, L.-M.; Li, Y.-F.; Mi, W.-D. Deferoxamine attenuates lipopolysaccharide-induced neuroinflammation and memory impairment in mice. *J. Neuroinflamm.* **2015**, *12*, 1–13. [[CrossRef](#)] [[PubMed](#)]
49. Al-Dabbagh, B.; Elhaty, I.A.; Murali, C.; Al Madhoun, A.; Amin, A. *Salvadora persica* (Miswak): Antioxidant and promising antiangiogenic insights. *Am. J. Plant Sci.* **2018**, *9*, 1228. [[CrossRef](#)]
50. Beurel, E.; Jope, R.S. Lipopolysaccharide-induced interleukin-6 production is controlled by glycogen synthase kinase-3 and STAT3 in the brain. *J. Neuroinflamm.* **2009**, *6*, 1–11. [[CrossRef](#)]
51. Yu, K.; Ma, Y.; Li, X.; Wu, X.; Liu, W.; Li, X.; Shen, J.; Wang, H. Lipopolysaccharide increases IL-6 secretion via activation of the ERK1/2 signaling pathway to up-regulate RANKL gene expression in MLO-Y4 cells. *Cell Biol. Int.* **2017**, *41*, 84–92. [[CrossRef](#)]
52. Chu, X.; Zhou, S.; Sun, R.; Wang, L.; Xing, C.; Liang, R.; Kong, Q. Chrysophanol relieves cognition deficits and neuronal loss through inhibition of inflammation in diabetic mice. *Neurochem. Res.* **2018**, *43*, 972–983. [[CrossRef](#)]
53. MacPherson, K.P.; Sompol, P.; Kannarkat, G.T.; Chang, J.; Sniffen, L.; Wildner, M.E.; Norris, C.M.; Tansey, M.G. Peripheral administration of the soluble TNF inhibitor XPro1595 modifies brain immune cell profiles, decreases beta-amyloid plaque load, and rescues impaired long-term potentiation in 5xFAD mice. *Neurobiol. Dis.* **2017**, *102*, 81–95. [[CrossRef](#)]
54. Means, J.C.; Gerdes, B.C.; Kaja, S.; Sumien, N.; Payne, A.J.; Stark, D.A.; Borden, P.K.; Price, J.L.; Koulen, P. Caspase-3-dependent proteolytic cleavage of tau causes neurofibrillary tangles and results in cognitive impairment during normal aging. *Neurochem. Res.* **2016**, *41*, 2278–2288. [[CrossRef](#)]
55. Thakur, A.; Wang, X.; Siedlak, S.L.; Perry, G.; Smith, M.A.; Zhu, X. c-Jun phosphorylation in Alzheimer disease. *J. Neurosci. Res.* **2007**, *85*, 1668–1673. [[CrossRef](#)] [[PubMed](#)]
56. Waetzig, V.; Czeloth, K.; Hidding, U.; Mielke, K.; Kanzow, M.; Brecht, S.; Goetz, M.; Lucius, R.; Herdegen, T.; Hanisch, U.K. c-Jun N-terminal kinases (JNKs) mediate pro-inflammatory actions of microglia. *Glia* **2005**, *50*, 235–246. [[CrossRef](#)] [[PubMed](#)]
57. Attallah NG, M.; Negm, W.A.; Elekhawy, E.; Elmongy, E.I.; Altwaijry, N.; El-Haroun, H.; El-Masry, T.A.; El-Sherbeni, S.A. Elucidation of Phytochemical Content of *Cupressus macrocarpa* Leaves: In Vitro and In Vivo Antibacterial Effect against Methicillin-Resistant *Staphylococcus aureus* Clinical Isolates. *Antibiotics* **2021**, *10*, 890. [[CrossRef](#)] [[PubMed](#)]
58. Tsugawa, H.; Cajka, T.; Kind, T.; Ma, Y.; Higgins, B.; Ikeda, K.; Kanazawa, M.; VanderGheynst, J.; Fiehn, O.; Arita, M. MS-DIAL: Data-independent MS/MS deconvolution for comprehensive metabolome analysis. *Nat. Methods* **2015**, *12*, 523–526. [[CrossRef](#)]
59. Attallah, N.G.; El-Kadem, A.H.; Negm, W.A.; Elekhawy, E.; El-Masry, T.A.; Elmongy, E.I.; Altwaijry, N.; Alanazi, A.S.; Al-Hamoud, G.A.; Ragab, A.E. Promising Antiviral Activity of *Agrimonia pilosa* Phytochemicals against Severe Acute Respiratory Syndrome Coronavirus 2 Supported with In Vivo Mice Study. *Pharmaceuticals* **2021**, *14*, 1313. [[CrossRef](#)]
60. Alotaibi, B.; Negm, W.A.; Elekhawy, E.; El-Masry, T.A.; Elseady, W.S.; Saleh, A.; Alotaibi, K.N.; El-Sherbeni, S.A. Antibacterial, Immunomodulatory, and Lung Protective Effects of *Boswellia dalzielii* Oleoresin Ethanol Extract in Pulmonary Diseases: In Vitro and In Vivo Studies. *Antibiotics* **2021**, *10*, 1444. [[CrossRef](#)]
61. Alotaibi, B.; Negm, W.A.; Elekhawy, E.; El-Masry, T.A.; Elharty, M.E.; Saleh, A.; Abdelkader, D.H.; Mokhtar, F.A. Antibacterial activity of nano zinc oxide green-synthesised from *Gardenia thailandica* triveng. Leaves against *Pseudomonas aeruginosa* clinical isolates: In vitro and in vivo study. *Artif. Cells Nanomed. Biotechnol.* **2022**, *50*, 96–106. [[CrossRef](#)]
62. Jin, Y.; Peng, J.; Wang, X.; Zhang, D.; Wang, T. Ameliorative effect of ginsenoside Rg1 on lipopolysaccharide-induced cognitive impairment: Role of cholinergic system. *Neurochem. Res.* **2017**, *42*, 1299–1307. [[CrossRef](#)]
63. Ohkawa, H.; Ohishi, N.; Yagi, K. Assay for lipid peroxides in animal tissues by thiobarbituric acid reaction. *Anal. Biochem.* **1979**, *95*, 351–358. [[CrossRef](#)]
64. Nandi, A.; Chatterjee, I. Assay of superoxide dismutase activity in animal tissues. *J. Biosci.* **1988**, *13*, 305–315. [[CrossRef](#)]
65. Aebi, H. Catalase in vitro. In *Methods in Enzymology*; Elsevier: Amsterdam, The Netherlands, 1984; Volume 105, pp. 121–126.
66. Freeman, W.M.; Walker, S.J.; Vrana, K.E. Quantitative RT-PCR: Pitfalls and potential. *Biotechniques* **1999**, *26*, 112–125. [[CrossRef](#)] [[PubMed](#)]

67. Livak, K.J.; Schmittgen, T.D. Analysis of relative gene expression data using real-time quantitative PCR and the $2^{-\Delta\Delta CT}$ method. *Methods* **2001**, *25*, 402–408. [[CrossRef](#)] [[PubMed](#)]
68. Negm, W.A.; El-Kadem, A.H.; Elekhawy, E.; Attallah, N.G.; Al-Hamoud, G.A.; El-Masry, T.A.; Zayed, A. Wound-healing potential of rhoifolin-rich fraction isolated from *Sanguisorba officinalis* roots supported by enhancing re-epithelization, angiogenesis, anti-inflammatory, and antimicrobial effects. *Pharmaceuticals* **2022**, *15*, 178. [[CrossRef](#)] [[PubMed](#)]

Disclaimer/Publisher's Note: The statements, opinions and data contained in all publications are solely those of the individual author(s) and contributor(s) and not of MDPI and/or the editor(s). MDPI and/or the editor(s) disclaim responsibility for any injury to people or property resulting from any ideas, methods, instructions or products referred to in the content.